THE PENNSYLVANIA STATE UNIVERSITY
SCHREYER HONORS COLLEGE

DEPARTMENT OF MECHANICAL ENGINEERING

DETERMINATION OF DEPLOYABLE TRANSDUCER ARRAY DIMENSIONS FOR TREATING OCULAR MELANOMAS

NICHOLAS MOORE
SPRING 2022

A thesis
submitted in partial fulfillment
of the requirements
for a baccalaureate degree
in Mechanical Engineering
with honors in Mechanical Engineering

Reviewed and approved* by the following:

Ryan Harne, PhD.
James F. Will Career Development Associate Professor
Thesis Supervisor

Daniel Cortes, PhD.
Assistant Professor of Mechanical Engineering
Honors Adviser

* Electronic approvals are on file.

ABSTRACT

One promising new treatment method for solid tumors uses high intensity focused ultrasound, or HIFU, generated from a transducer array to focus a necessary acoustic pressure at the site of the tumor to induce thermal ablation [1]. In current operation, these transducer arrays are large and extracorporeal, limiting the treatment to tumors that are not deep within the body [1]. This project is focused on negating the drawbacks of current HIFU treatments by developing the design parameters for a smaller, foldable array that can be implanted within the body using laparoscopic surgery to treat ocular melanomas. This process increases the proximity of the array to tumors deep within the body so that they can be treated with this new procedure.

One candidate for an array design uses a tessellated Miura-ori geometry to mimic the shape of a hemisphere. Using an analytical model that predicts the acoustic pressure generated by the array design and the subsequent thermal rises attributed, the efficacy of a given design for treating ocular melanomas can be determined. Using the same method, it was first determined that an ideal arc transducer had the ability to achieve necessary focusing to thermally ablate a tumor comparable to an ocular melanoma. After proving the ability of transducer arrays to treat these solid tumors, tailoring the dimensions, driving power, and positioning of the Miura-ori array through parametric investigation determined that a Miura-ori tessellated geometry mimicking that of an ideal arc transducer is able to achieve necessary focusing for ocular melanoma treatment. With these determined design parameters, a prototype HIFU probe can be manufactured by external collaborators and used in pre-clinical testing.

TABLE OF CONTENTS

LIST OF FIGURES

LIST OF TABLES

ACKNOWLEDGEMENTS

I would like to thank my thesis supervisor Dr. Ryan Harne for his continued support and guidance throughout the entirety of the thesis research/writing process. Dr. Harne took me into his research lab with no prior knowledge of acoustics and a very basic skillset in MATLAB and taught me how to apply a structured research process to tackle engineering problems that would have seemed impossibly complex previously. For that I am very grateful. I would also like to thank my honors advisor Dr. Daniel Cortes for his support as my secondary thesis reader and for guiding me throughout my four years of college. Finally, I would like to thank my family and friends for their unconditional support. I would not be here without them.

Chapter 1

BACKGROUND

Over the past two hundred years, the world has seen great advancements in medicine. From penicillin to anesthesia, organ transplants to stem cell therapy, the medical discoveries since germ theory (discovery of microscopic bacteria and viruses) have drastically improved the standard of life for humankind. However, there is one disease that remains a pressing issue across the globe: cancer.

Currently, the main method of treating solid tumors is open surgery, which can be used exclusively or coupled with chemotherapy or radiotherapy [1]. However, these treatments have many drawbacks that reduce the quality of life of the cancer patients. For example, patients often fear invasive surgery due to its possible complications, such as substantial pain, immunosuppression, a lengthy recovery, and sometimes death [1]. Even treatments like chemotherapy and radiotherapy possess potential serious side effects. Radiotherapy operations like radiofrequency ablation can lead to metastasis attributed to tumor seeding, a process where malignant cancer cells are moved to another area of the body along the needle track [1].

Introduction to HIFU Methodologies

The risky treatment methods for solid tumors necessitate a new form of treatment that is less invasive, less hazardous, but equally effective. One promising therapy involves a non-invasive surgery using high intensity focused ultrasound, or HIFU [1]. This treatment method works to destroy the cancer from outside the body by focusing ultrasound at the tumor to produce the necessary acoustic power to thermally ablate the diseased tissue [2]. This process is called coagulative necrosis and occurs when tissue is exposed to large amounts of acoustic pressure under a short amount of time, producing enough thermal energy to effectively destroy the tissue [2]. This HIFU is produced due to transducers that oscillate a piezoelectric material by applying an alternating voltage, which are structured in a curved array to harness focusing abilities [1], [2]. Two different HIFU methods are most often used for thermally ablating tissue. The first has a curved, out-of-body transducer focusing acoustic pressure at the entire solid tumor, while the second attempts to "paint" out a solid tumor by destroying successive sections of the tissue [1].

HIFU is a promising new treatment method that works to accomplish the same goals as pre-existing methods, while eliminating the risks that the traditional treatments pose. HIFU procedures have already been used to effectively treat organ-confined prostate, liver, breast, kidney, sarcoma, and uterine fibroid cancers without the complications of traditional treatments [1]. Further, it does not impair the immune system, has lower side effects, less pain, can be used for any tissue type, can be done repeatedly (repeated ultrasound exposure is safe for the body), and has not been shown to increase risk of metastasis [1].

Although the number of patient benefits of HIFU treatments are large, drawbacks remain with this new procedure. There have been reported cases of reflected ultrasound causing skin burns above the treatment area [2]. Additionally, these transducers have limitations in the treatment of some tumors. For example, tumors deep within the body are hard to treat with ultrasound because it is reflected at tissue interfaces, is attenuated by bone, and cannot be done through air. This makes tumors in the lungs, bowel, ribs, and skull impossible to treat [1], [2].

Even with these limitations, the clinical applications and benefits that HIFU provides make it a promising new treatment method that could become as common as surgery with technological advances in the transducer equipment [1], [2].

One possible method of combating these drawbacks is to use origami-inspired foldable transducer arrays that can be deployed into the body to reduce the distance between the transducer and target area, minimizing the limitations caused by reflection and attenuation. This would work by having a fully folded array form that can be deployed into the body using laparoscopic surgery, which would unfold into its functional form once it is in the correct position for treatment [3].

Miura-Ori Geometry

Another possible base unit is called the Miura-Ori tessellation. This unit has been studied extensively for wave guiding transducer arrays due to its ease of manufacturing and wide variety of industrial applications [4]. This tessellation is composed of four adjacent parallelograms that can fold along its edges, with the exact shape and size of each tessellation unit being described by four parameters: edge lengths a and b, edge angle γ, and folding angle Θ [5].

In order to determine the appropriate base unit and parameter values, it is imperative that the wave focusing abilities of the transducer array can be quantified. In the analytical framework, the point $p(R,\beta,\phi)$ in spherical coordinates represents the pressure change at any point in space that is produced by the summation of the superimposed acoustic waves generated by each transducer in the array, if the left vertex of the array is placed at the origin [5]. In this framework, R refers to the magnitude of the distance from the origin to the point, β defines the polar angle measured from the z-axis, and ϕ defines the azimuthal angle measured from the x-axis. In an Ohio State University study on the use of Miura-Ori tessellations for foldable transducer arrays, an analytical model that had the ability to calculate the acoustic pressure generated at any point was established and experimentally verified [5]. The results of this research confirmed the elite wave guiding abilities of the Miura-Ori unit and called for an advancement of the acoustic pressure modeling in order to better understand its total range of applications [5]. However, inconsistencies were found in the near-field model predictions that resulted from inaccuracies in the manufacturing of the transducers. With advancements in manufacturing, it is hoped that this shortcoming can be negated [5].

The creation and advancement of acoustic pressure modeling is essential for the design of a transducer array that will optimize wave focusing properties. Arrays that produce HIFU use phase delays to manipulate the constructive and destructive interferences between the waves generated by each individual transducer to focus acoustic pressure [3]. In another Ohio State University study, an iterative design process to create foldable arrays to focus acoustic energy is established, where different folding angles can be used to adjust focusing ability based on the interference in different scenarios [3]. The design process itself is founded on the ability to create accurate boundary element modeling to calculate produced acoustic pressure for arbitrary base units. By studying the acoustic fields generated, the optimal array parameters can be found.

Analytical Modeling of Acoustic Pressure Field

These generated fields can also be used to determine the relationships between the array parameters and the characteristics of the fields themselves. Advancements in modeling take into account how exactly the diffracted and reflected waves sum to form the total acoustic pressure at the focal point. To do this, the acoustic pressure due to direct radiation was calculated using Rayleigh's integral at the arbitrary point p(R,β,ϕ) (see figure 2) [5]. Integrals are then determined for modeling the effects of both wave reflection and diffraction that occur at neighboring facets in the array [6]. By summing all of these factors, the total acoustic field emitted from a Miura-ori array can be determined through modeling that has been experimentally verified [6]. It is found that reflections contribute more if the intended receiving point is at the broadside, or perpendicular to the array, while diffraction gains a larger influence if the receiving point is at the endfire, or parallel along the axis of the array [6].

Although the model based solely on direct radiation, reflection, and diffraction produced experimentally verified acoustic fields, it failed to take into account if the generated ultrasound travels through different media. In an application of foldable transducer arrays to thermally ablate solid tumors, there are different tissue types that the ultrasound must travel through before it reaches its receiving point. Reflection, refraction, and attenuation can all occur at the interfaces between different materials, which will disrupt the total acoustic field at the focal point. In a study of deployable transducer arrays in multilayer environments, Harne and Zou develop an even more accurate analytical model by applying Rayleigh's integral at the interface between two media based on array dimensions, positioning, and driving power [6]. To do this the interface is discretized, with each individual discretized contribution being superimposed to calculate total transmitted and reflected acoustic pressures from the interface [7]. This method of discretization developed by Ocheltree and Frizzell breaks down each parallelogram subfacet of the array into two triangles, with each successive mesh refinement breaking down each triangle into four smaller triangles [7]. This method is applied to both the interfaces and the array surface

[6]. These pressures can then be applied in the steady state solution of the bio-heat transfer model to determine the heat generated due to ultrasound at the focal point of the array by discretizing the tissue layers into volumetric elements and superposing their thermal contributions [6], [8]. The thermal contributions from each volume on an arbitrary point were determined from Nyborg's solution of the bio-heat transfer model for a "step-function point source" [9]. This determination of generated heat is especially important for the design of a foldable transducer array because it will establish whether the acoustic pressure generated is enough to thermally ablate the diseased tissue. In this study, the efficacy of this analytical model was experimentally verified by comparing its results to that of direct numerical simulations using finite element analysis, and concluded that a foldable, Miura-ori transducer array has the ability to produce enough heat to induce cell death [7].

The comprehensive model produced by Harne and Zou also led to discoveries in the relationships between some key array parameters and the generated acoustic pressures. For one, the f-number (ratio of focal length to aperture size) is directly related to a transducer's ability to focus ultrasound [7]. A lower f-number relates to a greater frequency and concentration of ultrasound at the focal point [7]. Other important design findings are that increases in the width of the array (number of base units in the y-axis) reduce focusing capabilities, and that the second edge angle γ_2 has an influence on the location of the maximum pressure amplitude [7]. The research into parameter influences has been furthered by Zhao in a study of sound focusing by reconfigurable acoustic arrays. The research concluded that a greater activation of the surfaces will produce a greater acoustic pressure, and that partially activated arrays produce less destructive interference [10]. By using the comprehensive analytical model determined by Harne and Zou and the relationships between array parameters and generated acoustic pressures, there is a possibility of determining the optimal parameter values for applications in solid tumor treatment.

FDA Regulations for HIFU

When a new medical device or technology is developed, it first must be approved by the U.S. Food and Drug Administration, or FDA. This approval process confirms that the new device meets an FDA determined safety and efficacy level as described in the Medical Device Amendments to the U.S. Food, Drug, and Cosmetic Act (1976) [11]. This legislation categorizes all medical devices into either Class I, Class II, or Class III, where there is increasing risk with each successive class. HIFU technology has previously been classified as both Class II or Class III since it is a newer technology with many unknown risks, but there has yet to be a generalized set of standards for HIFU due to this lack of knowledge [11]. The deployable HIFU transducer array that is studied within this project would most likely be classified as a Class III medical device as it has yet to undergo preclinical testing and would be used to treat tumors deep within the body.

Although new HIFU technologies do not have solidified regulation requirements and are usually judged on a case-by-case basis, there are multiple methods of assessing the risk of a new device. One of the most widely used methods for risk assessment before a prototype is generated is computational modeling [11]. As previously discussed in the Analytical Modeling of Acoustic Pressure section, the acoustic pressure field generated by a Miura-ori tessellated array can be predicted from the array geometry, driving frequency, and positioning using computational modeling. These acoustic pressure amplitudes can then be used with the bio-heat transfer model to predict the temperature rises at any point within the tissue [8]. Since the goal of HIFU cancer treatments are to thermally ablate the tumor while leaving neighboring tissue undamaged, a plot of the thermal rises throughout the tissue and tumor can be used to determine if there is a temperature rise great enough to induce cellular necrosis outside of the target area. Additionally, the velocity vectors of the waves generated can be used with the pressure amplitudes to determine a distribution of the acoustic intensity throughout the tissue.

The goal of this thesis is to determine designs for foldable HIFU transducers to be used to treat ocular melanomas. By tailoring the dimensions, driving power, and positioning of the transducer via parametric investigations, this research will identify candidate implementations of the transducers that deliver the necessary acoustic power to the focal point where the malignant tissues will be thermally ablated. In an application of treating ocular melanomas, there is a critical need to determine the folding HIFU transducer dimensions, driving power, and positioning in order to destroy the malignant tissues inside the eye. By determining these key parameters, a proof-of-concept HIFU probe may be developed by external collaborators and used in pre-clinical testing trials. To accomplish this, the objective of this research is to use an analytical model to determine the optimal dimensions, driving power, and positioning of a foldable, deployable transducer array to produce the required acoustic pressure at a focal point to thermally ablate diseased tissue. Using the bio-heat transfer equation in tandem with a model that predicts acoustic power radiated from a folding transducer, the optimized sound field will be examined in relation to the ability to control cell necrosis for ocular necrosis treatments.

Chapter 2

METHODS

The optimal design of the transducer array geometry and driving frequency were determined using parametric investigation via computational analysis in MATLAB. Thus the methodology of this project is not a lab procedure, but rather the analytical modeling framework used to predict the acoustic pressure field, temperature rises, and acoustic intensity magnitudes generated by the array geometry and driving frequency being tested. The modeling and mesh generation used for predicting the acoustic pressure field and temperature rises generated from a Miura-Ori tessellation was developed by R. Harne and C. Zou of Ohio State University for arrays of equal numbers of transducers per row [5]. This mesh generation was slightly altered in this project so that arrays with unequal row lengths could be tested.

To determine if a transducer array could produce the necessary focusing to thermally ablate an ocular melanoma without harming the rest of the eye, the acoustic pressure field and thermal rises generated from an ideal transducer arc through layers of water, sclera, and tumor were predicted. This was accomplished by combining the mesh generation of an ideal arc transducer with the analytical framework developed by R. Harne and C. Zou for predicting the acoustic pressures and thermal rises through multiple layers of different acoustic and thermal properties [6].

Once a satisfactory design was found, the acoustic intensity magnitudes were determined to ensure that they meet the FDA set regulations for HIFU technology. The acoustic intensity field was predicted from the determined acoustic pressure and wave velocity at each node. The wave velocity at each node was determined using finite difference method and was calculated from the pressure differences at adjacent nodes. The analytical framework used to determine the acoustic pressure field, thermal rises, and acoustic intensity magnitudes for Miura-Ori tessellations and ideal arc transducers are discussed in more detail in each section of this chapter.

Alteration of Miura-Ori Mesh Generation

To model Miura-Ori arrays of different row lengths, the modeling framework used by Harne and Zou for predicting the acoustic field and thermal rises from a rectangular Miura-Ori array had to be altered. This alteration was a relatively simple fix as only the modeling of the array geometry had to be changed, while the analytical modeling framework for calculating the acoustic pressure field and thermal rises from the array geometry remained unaffected.

This geometrical modeling method uses the independent structural parameters edge lengths a and b, edge angles γ_1 and γ_2, and folding angle Θ to define the spatial extents of a folded, Miura-Ori unit cell [12]. The spatial extents H, S, L, and V were derived by Schenk and Guest to easily map the positions of the nine vertices of a Miura-Ori unit, and are defined as such: $H = a \sin\theta \sin\gamma$, $S = b\frac{\cos\theta \tan\gamma}{\sqrt{1+(\cos\theta)^2(\tan\gamma)^2}}$, $L = a\sqrt{1-(\sin\theta\sin\gamma)^2}$, $V = b\frac{1}{\sqrt{1+(\cos\theta\tan\gamma)^2}}$ [13].

These spatial extents and vertex positions were used to calculate the center and radii of two arcs used to model the geometry of the folded unit [12]. The arcs are defined by the three vertices that lie across its span.

The radii and center points of both arcs are then used to calculate the chord lengths between the vertices and the radius angles of these chords, which are used to calculate the nodes of the folded, Miura-Ori unit cell that are used in the acoustic pressure computations [12]. To model arrays of differing units, this methodology is applied successively to model each individual unit via for loops and if statements. In this way, an if statement was used to denote the number of units per row while the for loop modeled each folded, Miura-Ori unit of each row in succession. By varying the number of units per row, a Miura-Ori structure that resembles a hemispherical shape with enhanced focusing can be modeled and its generated acoustic pressure and thermal fields predicted using the same analytical framework used by Harne and Zou. In the figure below, an example hemispherical Miura-Ori structure can be seen.

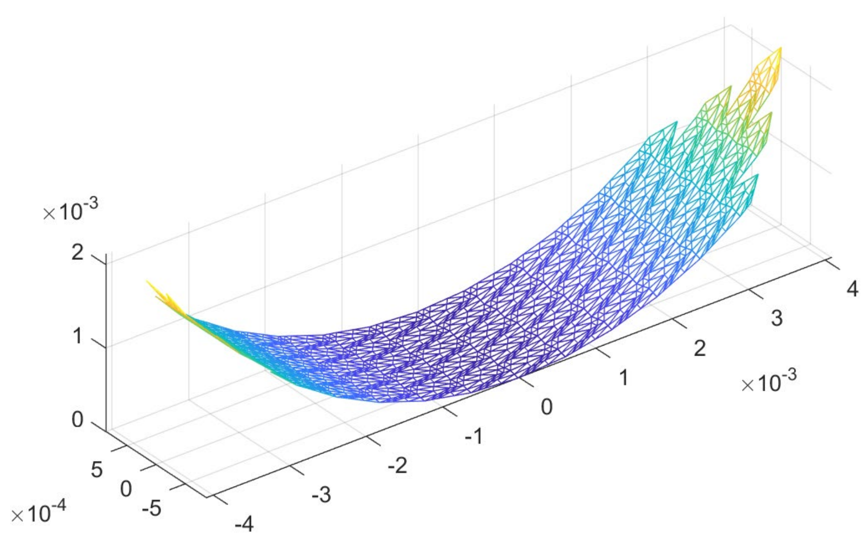

Figure 1. Example Hemispherical Miura-Ori Structure

Analytical Modeling of Ideal Arc Transducer

Ideal arc transducers are theoretical devices composed of a hemispherical surface with an infinite number of point sources emitting ultrasound along its surface. These ideal arc transducers are useful for predicting the most ideal focusing of a Miura-Ori transducer array because they mimic the curved shape of the array in its unfolded, functional form [6].

Similar to the alteration of the rectangular Miura-Ori modeling, Harne and Zou's method of predicting the acoustic pressure field and thermal rises generated from a transducer array in a multilayer environment was used for the ideal arc transducer. The only thing that needed to be changed was the geometric modeling and mesh generation. This came from Harne and Zou's previous investigation of ideal arc transducers and their predicted generated acoustic pressure field through a single layer environment [12]. However, this model did not have the capability of predicting the thermal rises generated by these ideal transducers, nor could it incorporate a multilayer environment. Thus, the geometric modeling and mesh generation of the ideal arc transducer was imported into the model for predicting the acoustic pressure field and thermal rises through multilayer media for Miura-Ori arrays. This was possible because both models used the same discretization method developed by Ocheltree and Frizzell [7]. The geometric model for the ideal transducer placed the focal point of the arc at the origin, while the Miura-Ori model performed computational analysis for an array that was positioned at the origin. To unite the two models, the nodes determined from the ideal arc transducer mesh generation are translated in the z-axis by the length of the radius of curvature of the arc. In the figure below, a sample ideal arc transducer structure formed by this geometric model is displayed.

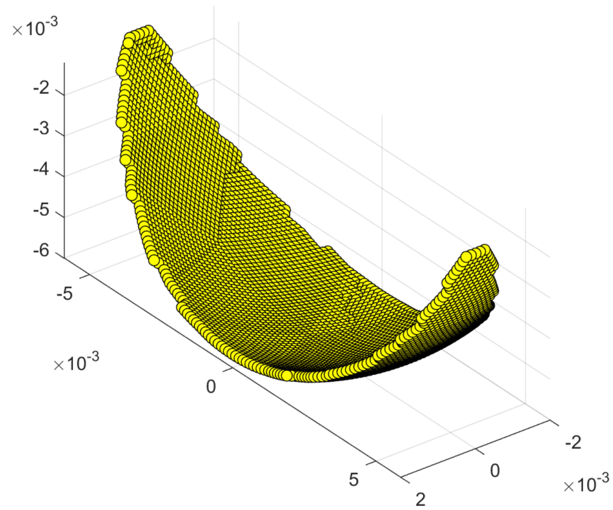

Figure 2. Ideal Arc Transducer Structure

In the figure above, the scale for each axis is in meters multiplied by the scale factor listed. Thus, the tick marks on each axis represent millimeters in length. The structure of the arc is defined by a set of parameters that include the sphere angle, the radius of curvature, and the two scribe angles. The scribe angles define the span of the sphere that the transducer encompasses in the x and y directions (with the z-axis plotted vertically), while the sphere angle defines the part of the sphere encompassed by the transducer surface [12]. The radius of curvature sets the focal point of the arc. For a more visual representation of what each parameter defines, see Appendix figures A.1-4.

Determination of Acoustic Intensity Field

The model used to determine the acoustic intensity field calculated the acoustic intensity magnitude at every node as a function of the acoustic pressure and wave velocity at each node. The acoustic pressure values are determined from the predicted acoustic pressure field discussed in both the Analytical Modeling of Acoustic Pressure Field section of the Introduction and the Alteration of Miura-Ori Analytical Model section of the Methods. The wave velocity at each node is determined as a function of the acoustic pressure difference across adjacent nodes, the driving frequency of the transducer array ω, and the density of the tissue the nodes reside in ρ. This determination considers the span between two adjacent nodes as a one-dimensional duct filled with air with a harmonically vibrating piston at one end. The displacement of the piston can be described as $d(t) = De^{j\omega}$. Differentiating this equation with respect to time yields the velocity of the waves generated by the piston at the boundary between piston and air $u(0,t) = j\omega De^{j\omega}$, assuming that the wave velocity of the boundary is equal to the piston velocity [14]. This wave velocity boundary condition is used with Euler's equation relating pressure changes over distance to changes in wave velocity with respect to time: $-\frac{\partial \rho}{\partial x} = \rho \frac{\partial u}{\partial t}$.

Differentiating the boundary condition returns $\frac{\partial u}{\partial t} = j\omega(j\omega De^{j\omega})$, or essentially $\frac{\partial u}{\partial t} = j\omega(u(0,t)$. Substituting this expression into Euler's equation and solving for u(0,t) produces the model used to predict the wave velocity at each node as a complex conjugate: $u(0,t) = \frac{-1}{\rho\omega j}\frac{\partial \rho}{\partial x}$.

Using one-dimensional finite difference method, the wave velocity can be calculated at all but the last node, as there is no calculable pressure change. δp is calculated as the pressure difference between the node whose wave velocity is being calculated and the successive node, with δx being the distance between the two nodes. This finite difference method is applied across the x, y, and z directions to determine the x, y, and z components of the wave velocity at each node. The acoustic intensity is then calculated as a product of the nodal acoustic pressure and wave velocity: $I = \frac{1}{2}Re[pu]$.

In this expression I is the one-dimensional, time-harmonic average intensity component and u is the wave velocity as a complex conjugate [14]. Calculating I in x, y, and z can be summed to determine the acoustic intensity magnitude at every node within the acoustic pressure field.

Chapter 3

RESULTS

In order to determine the optimal design parameters for a tessellated Miura-Ori transducer array, multiple different groups of designs needed to be tested to achieve the focusing necessary for successful ocular melanoma treatment. The design process began with the analytical framework and mesh generation used by R. Harne and C. Zou for predicting the acoustic pressure field and thermal rises generated by a Miura-Ori array [5]. The arrays tested in this phase of the design process had an equal number of transducer units per row (as described in Alteration of Miura-Ori Mesh Generation in Chapter 2 METHODS). After varying the structural parameters and driving frequency, it became clear that a Miura-Ori array of equal row units would not achieve necessary focusing to ablate an ocular melanoma without harming the rest of the eye. This lack of focusing ability created a need to determine if a transducer array design with optimal focusing was even possible. Thus, ideal arc transducers were tested under the same conditions using the combined ideal arc transducer mesh and multilayer code as outlined in Analytical Modeling of Ideal Arc Transducer in Ch. 2 METHODS. Although ideal arc transducers are theoretical, this stage of testing would determine the maximum upper bound on an array's focusing ability. The results of these tests generated acoustic pressure fields and thermal rises that displayed the necessary focusing for ocular melanoma treatment, proving that a successful array design was not impossible.

The next phase of the design process tested Miura-Ori arrays of different row lengths. As described in Alteration of Miura-Ori Mesh Generation in Chapter 2 METHODS, these new arrays mimicked the hemispherical shape of an ideal arc transducer with the center row having the most units and each successive row having two less units. After parametric investigations of this new array structure, designs with optimal focusing were achieved.

In this manner, the results of each stage of the design process determined the constraints and needs of the next stage. In this Chapter the results and interpretations of each stage of the design process are discussed in more detail, as well as a discussion of proposed further study.

Results of Rectangular Miura-Ori Structures

The rectangular Miura-Ori structures were tested in a manner to simulate the operating conditions of a transducer array treating ocular melanomas. The ultrasound generated by these arrays must pass through a 3 mm thick layer of water, 1 mm thick layer of sclera, and 5 mm thick layer of tumor. These layers simulate the acoustic properties of the eye tissue affected by the HIFU generated by an array prototype and are used in calculating the acoustic pressure field through the three layers. The relevant acoustic properties of each layer are listed in the table below.

Table 1. Acoustic Properties of Water, Sclera, and Tumor

	Acoustic Properties		
Layer Material	**Attenuation Coefficient [Np/m/MHz]**	**Density [kg/m$^{3]}$**	**Speed of Sound [m/s]**
Water	0.00025328 [15]	997 [15]	1498 [15]
Sclera	10 [16]	1037 [16]	1618 [16]
Tumor	1 [17]	1030 [18]	1584 [17]

The scleral acoustic properties listed above were determined by Rohrbach, Ito, et al. in their investigation of the properties of human ocular tissue [16]. The attenuation coefficient and sound speed for a tumor were found from Tanoue, et al. via their investigation into prostate biopsy tissues using ultrasound speed microscopes [17]. Determining the thermal rises attributed to the acoustic pressure field required use of the bio-heat transfer model, which defines the temperature rise at any point as a function of the acoustic pressure and a range of tissue thermal properties [8]. These properties include perfusion rate, heat capacity, and thermal conductivity. The model takes into account the thermal properties of only the last layer (tumor) since most of the ultrasound is focused within this layer, and are listed in the table below [6].

Table 2. Thermal Properties of Tumor

Perfusion Rate [$m^3/m^3/s$]	**Heat Capacity [J/kg/K]**	**Thermal Conductivity [W/m/K]**
0.0063 [18]	3852 [18]	0.558 [18]

The thermal properties of the tumor, as well as its mass density, were determined by Çetingül and Herman's investigations of the thermal characteristics of melanoma lesions [18]. Considering the wide array of structural parameters used to define a Miura-Ori array, there is an infinite number of unique arrays that can be modeled. However, the number of possible structures that can be used for an application in ocular melanoma treatment are constrained by the eye dimensions and manufacturing limitations. In the figure below, a possible design of a folded, rectangular Miura-Ori array is pictured.

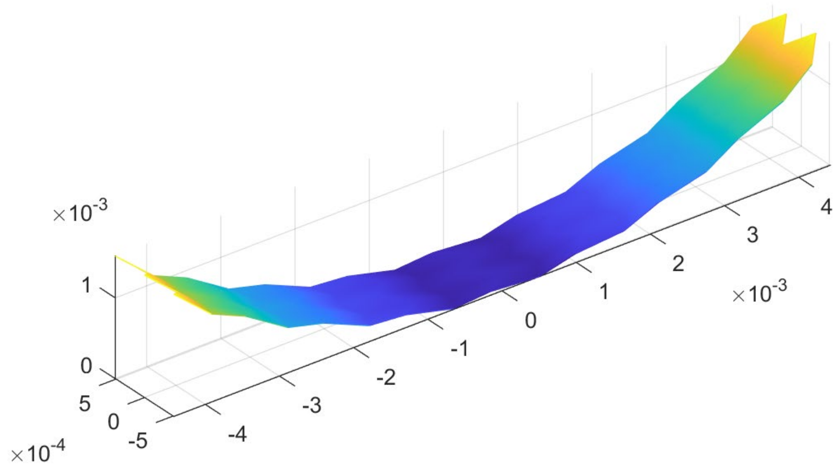

Figure 3. Rectangular Miura-Ori Array Structure

In this figure, the z direction is denoted by the vertical axis, the x direction is parallel to the span of the length of the array, and the y direction parallel to the width. Each tick mark of each axis represents a meter in length multiplied by the factor of ten with which it is labeled. The length of this folded, rectangular array spans approximately 8 millimeters, with a height of about 1.5 millimeters. The constraints imposed by the dimensions of the eye necessitate a maximum array span of 12 millimeters and a maximum height of 3 millimeters. Additionally, there are design constraints imposed on the folding angle of the array due to its heavy influence on the radius of curvature. This radius determines the focal point of the array where maximum peak pressure amplitude and thermal rise are achieved. In this application the focal point of the array should be positioned at about 6 millimeters above the origin, or about halfway through the tumor layer.

The final design itself must meet acoustic pressure field and thermal rise criteria to be considered a possible structure with ocular melanoma treatment capabilities. The peak thermal rise within the tumor must reach at least 10 Kelvin to induce cellular necrosis and thermally ablate the tumor [19].Further, this peak must be confined within a 2 mm gap with a thermal rise of no more than 4 Kelvin outside of this interval [19].This ensures that the tumor is ablated without harming the rest of the eye. Thus when analyzing the plots and data generated from tested rectangular Miura-Ori structures, the thermal rise plot along the z-axis is the most important for ensuring that the design meets the needed thermal criteria. The acoustic pressure amplitude plots are helpful for analyzing the distribution of pressure throughout the three layers. The acoustic pressure field for the tested rectangular array can be found in the Appendix (see A.5). When conducting parametric investigations into these rectangular arrays, one structural parameter is varied while the rest are held constant. Although this process was helpful for analyzing the effect of each parameter on the thermal distribution, the effects of these parameters are not independent. In other words, the changes in the thermal distribution resulting from a certain change in a structural parameter are not constant if other structural parameters are varied.

The results of parametric investigations of the rectangular Miura-Ori array produced no structures that met the necessary criteria for solid tumor treatment. Although these array structures produced the necessary acoustic pressure amplitude to induce a thermal rise of 10 K, the focusing capabilities did not meet the necessary criteria. For every rectangular array tested, the thermal rise was not contained within a 2 mm interval. In the figures below, an example structure is displayed with their corresponding thermal rise plots.

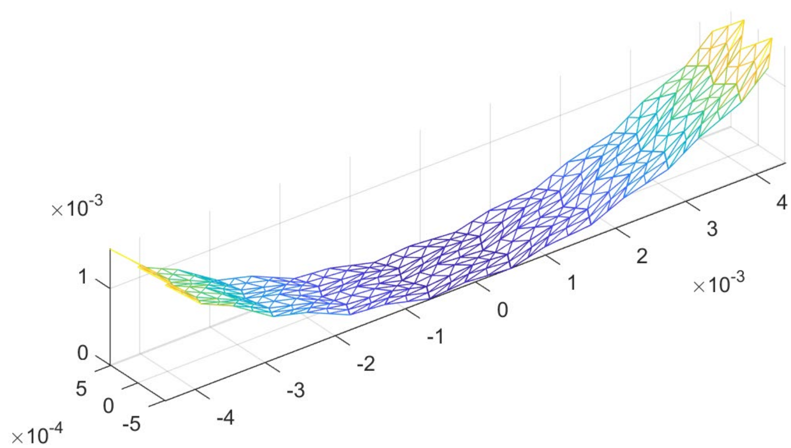

Figure 4. Example Tested Rectangular Miura-Ori Array

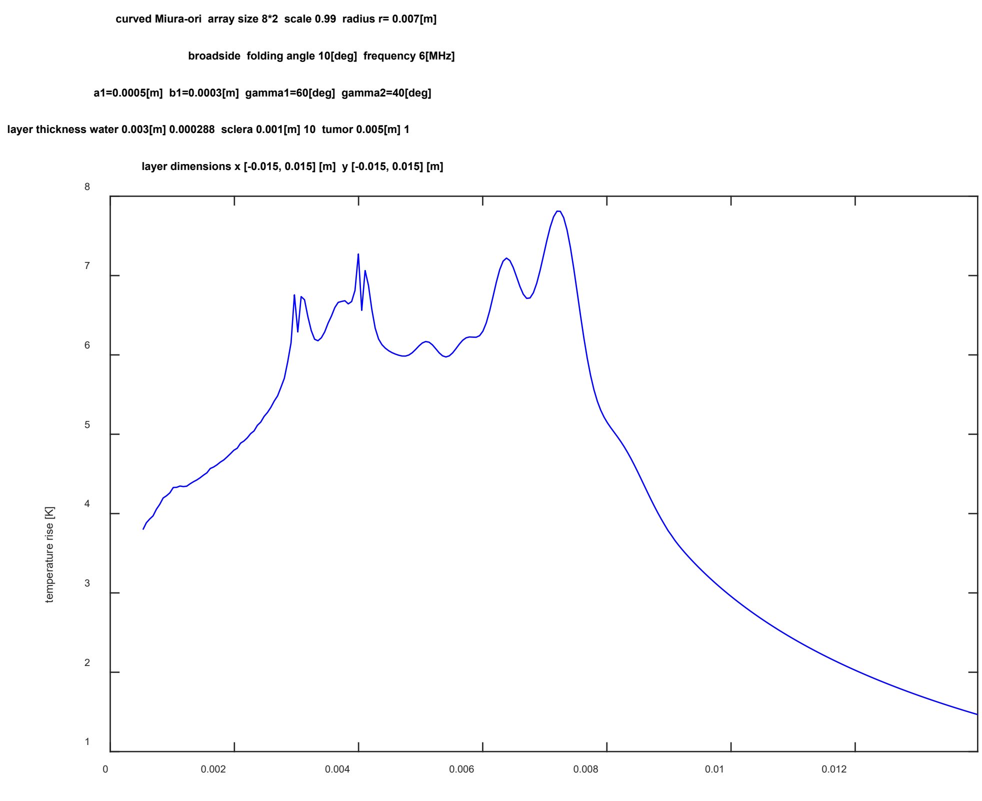

Figure 5. Thermal Rise Plot of Tested Rectangular Miura-Ori Array

The above structure contains 8 transducer units in length and 2 units in width, with edge angles of 60° and 40° and a folding angle of 10°. The edge lengths of the array were 0.5 millimeters and 0.3 millimeters, operating at a driving frequency of 6 MHz. In the thermal rise plot above, the peak thermal rise is approximately 7.8 K, with a thermal rise of about 7 K at the interface between the water and scleral layers (occurs at 4 millimeters on the z axis). Extrapolating this data for a peak thermal rise of 10 K would produce almost a 9 K temperature raise at the sclera. This estimation can be done because it was found through testing that adjusting the normal surface velocity of the transducers can alter the magnitude of the thermal rises without affecting focusing. This thermal rise would cause extensive damage to the scleral tissue and the rest of the eye, with this lack of focusing seen in all rectangular arrays analyzed by the computational modeling. With no possible successful designs generated for these particular arrays, a need was formed to determine if it is possible to treat ocular melanomas with a deployable transducer array.

Results of Ideal Arc Transducers

After merging the mesh generation of an ideal arc transducer with the analytical model predicting acoustic pressure fields and thermal rises for Miura-Ori arrays (as outlined in Analytical Modeling of Ideal Arc Transducer section of Chapter 2 METHODS), it was possible to determine if a transducer array could be designed with the ability of treating ocular melanomas. The simulations ran for these ideal arc transducers assumed the same operating conditions as for the rectangular Miura-Ori analysis: layers of water, sclera, and tumor of the same acoustic and thermal properties and thicknesses. The structure itself was constrained by the same length and height limitations as the rectangular Miura-Ori array. This was done so that the most ideal focusing in an ocular melanoma treatment application could be achieved and compared with the needs of the design to determine if a foldable, deployable transducer array had the ability to effectively treat ocular melanomas. In the figures below, the structure and thermal rises of an ideal arc transducer are displayed.

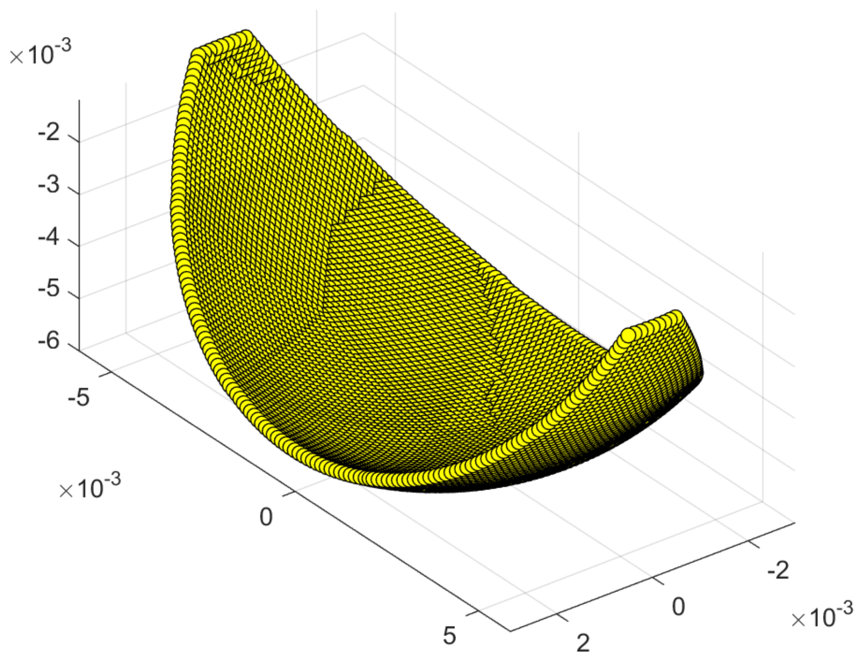

Figure 6. Tested Ideal Arc Transducer Structure

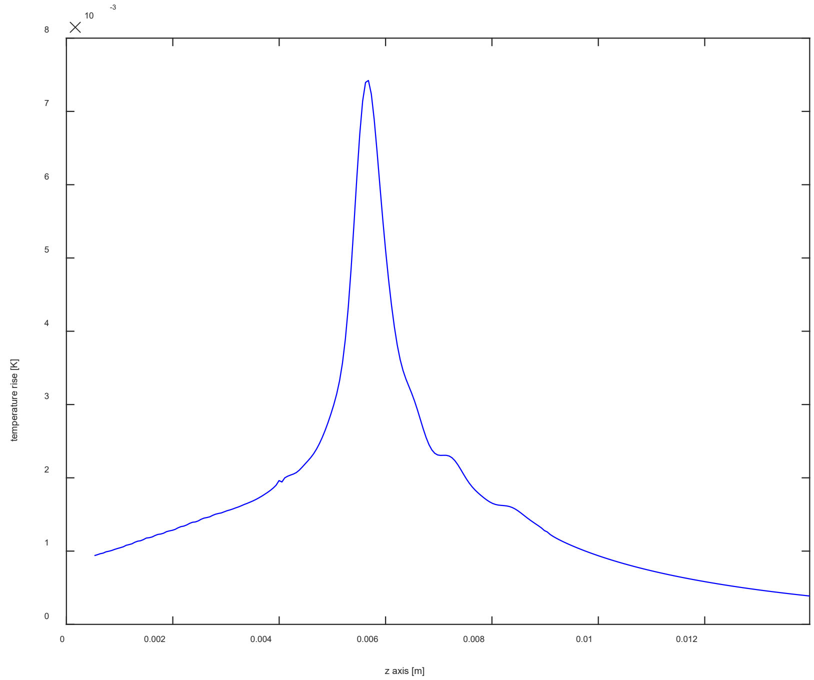

Figure 7. Predicted Thermal Rise for Tested Ideal Arc Array

The structural parameters for this tested ideal arc transducer are a sphere angle of 90 degrees, a radius of curvature of 6 millimeters, and scribe angles of 30 and 80 degrees operating at a driving frequency of 6 MHz. While the structure and predicted thermal rises generated are displayed above, the acoustic pressure field is located in the Appendix as it is not critical for determining the effectiveness of the array (see A.6). From the plotted thermal rises along the z-axis, a peak temperature increase of about 7.5 mK can be seen at a location of 6 millimeters - the radius of curvature of the array and thus the focal point. The interface between the sclera and tumor occurs at 4 mm along the z-axis and experiences a thermal rise of about 2 mK. Extrapolating these values for an ideal arc transducer array with a normal surface velocity that generates a 10 K peak thermal rise at the focal point, the peak thermal rise through the sclera would be about 2.67 K. According to the given design needs, this tested ideal arc transducer structure would be able to effectively treat ocular melanomas without harming the rest of the eye. Thus, this proves that it is not impossible to treat ocular melanomas with a foldable, deployable transducer array and creates a need for a model-able Miura-Ori array that mimics the hemispherical structure of an ideal arc transducer.

Results of Spherical Miura-Ori Arrays

As with the parametric investigations of the rectangular Miura-Ori arrays and the ideal arc transducers, the hemispherical Miura-Ori arrays were tested in the same multilayer environment. The results of the previous investigations were used to guide the selection of the hemispherical array parameters. For the rectangular Miura-Ori arrays, the tested designs that had folding angle to edge length ratios that produced a focal point at 6 mm were used as a benchmark for determining the hemispherical array edge lengths and folding angles. Furthermore, the investigations of the rectangular arrays showed that a driving frequency of 6 to 8 MHz tended to produce the best focusing capabilities, so most of the hemispherical arrays were tested at this operating condition.

The ideal arc transducer simulations helped to form the hypothesis that a Miura-Ori array would have the best focusing if it had the largest number of units at the smallest possible size. Ideal arc transducers emit ultrasound from an infinite amount of point sources located on its surface, which produces the cleanest constructive interference of ultrasound. Essentially this means that with the largest number of point sources, the focusing capabilities of an array are maximized. In terms of the application for treating ocular melanomas, this translates to reducing the edge lengths of the Miura-Ori units and increasing the number of units per row while ensuring that the structure meets the constraints imposed by the eye dimensions. From the results of the rectangular array investigations, this reduction in edge lengths also necessitated a decrease in the folding angle to maintain the correct focal length. In this way, the tests of the ideal arc transducer and rectangular arrays produced guiding constraints for the edge lengths, number of units, and folding angle of the hemispherical arrays for achieving the best possible focusing capabilities. In the figures below, the final design of the hemispherical array structure and its generated thermal rises are displayed.

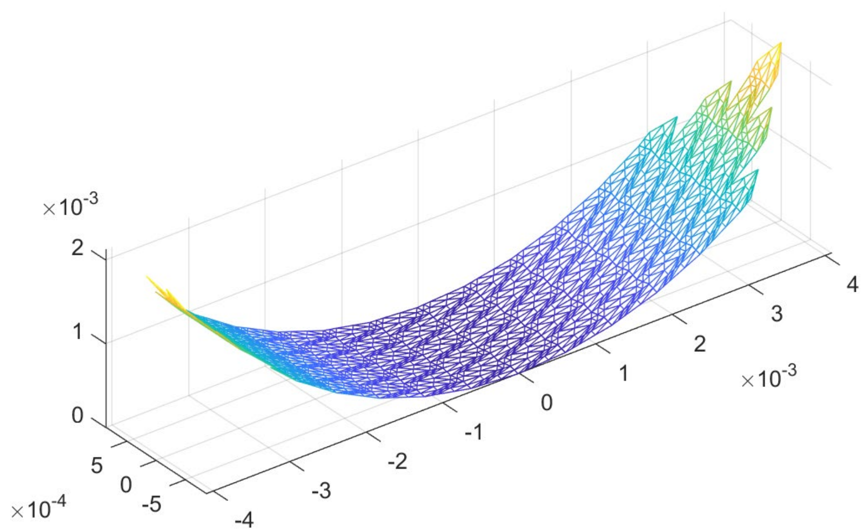

Figure 8. Structure of Final Design

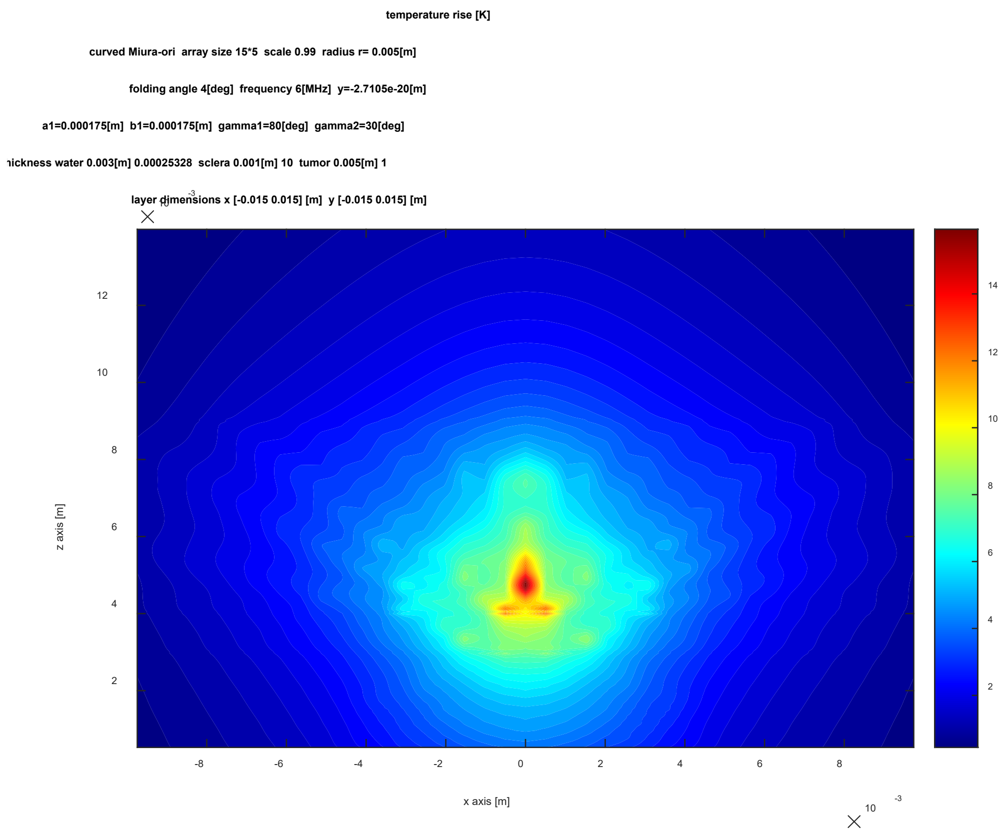

Figure 9. Generated Thermal Rise Contour for Final Design

The final design structure is a hemispherical Miura-Ori array of 5 rows. The center row has the most units at 15, with the adjacent rows having 13 units and the rows adjacent to them having 11 units. The edge lengths of the array are both .175 mm, the edge angles are 80° and 30° respectively, the folding angle is 4°, and it is operating at a driving frequency of 6 MHz. From the thermal rise contour above, the peak thermal rise is contained in a 0.5 mm span in the x-axis and a 1.5 mm span in the z-axis. This meets the criteria outlined in the Results of Rectangular Miura-Ori Structures section for safe ablation of ocular melanomas. The peak thermal rise at the focal point is approximately 16 K, which is considerably higher than the necessary thermal rise to induce cellular necrosis. However, the analytical framework used to predict the thermal rises in the tissue is a conservative model and may not account for all losses. These losses can include scattering or be produced by biological processes that are not accounted for. For example, blood has the ability to transfer heat away from the tumor as it flows through the body, which can reduce the magnitude of the peak thermal rise. This particular process is accounted for in the model via the perfusion rate of blood in the tumor, but similar biological processes like this could have the ability to produce unaccounted thermal losses. Therefore, the high thermal rises can be used to account for these losses. Additionally, the normal surface velocity of the transducers can be varied to produce the wanted thermal rise while maintaining focusing ability.

Once the final design was established, the model for predicting the acoustic intensities through the tissue had to be implemented to ensure the safety of the device. In the figure below, the acoustic intensity magnitudes are plotted along the z-axis.

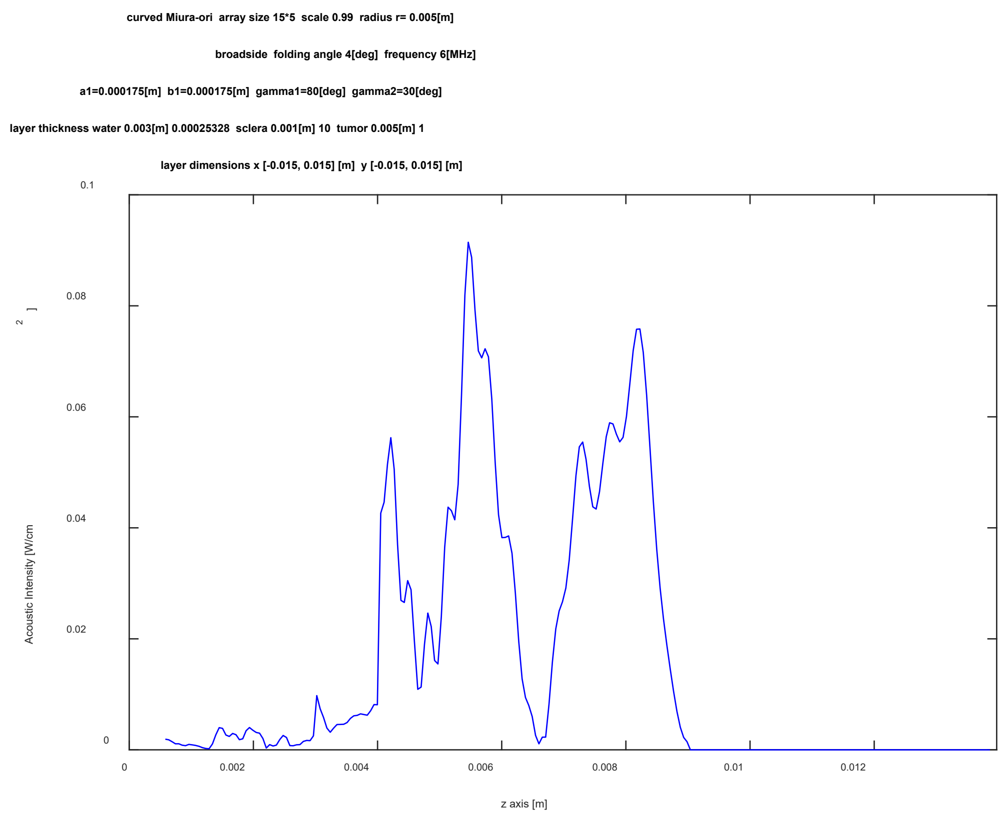

Figure 10. Generated Acoustic Intensity Magnitudes from Final Design

From the figure above, the acoustic intensity magnitudes reach their peak within the tumor at about 0.09 W/cm^2, and sharply decrease to approximately 0.01 W/cm^2 at the interface between the tumor and sclera (located at 0.004 m on the z-axis). Comparing these results with governmental regulations, in 1992 the FDA increased their temporal-average intensity limitations for ultrasound emitting devices to .72 W/cm^2 [20]. From the predicted generated acoustic intensity magnitude plots, the acoustic pressure field and thermal rises are deemed safe by FDA standards and are well within the regulation limits.

Discussion

Now that a design for a foldable, deployable Miura-Ori array that can safely and effectively ablate ocular melanomas has been established, the determined structure can move on to the next stage of the design process. With the design in place, it can be used as a guide for developing a prototype proof-of-concept probe to be used in pre-clinical testing. The final design has a maximum of 15 units per row, with 63 units in total. Considering that the curved array spans 8 mm in length, 1 mm in width, and has a radius of curvature of 5 mm, the width and length of each individual unit is .2 mm and 0.618 mm respectively. The length per unit was calculated from the arc length of the center row divided by the 15 units per row. Transducers of this size are incredibly difficult to manufacture and are costly and time-consuming. Further, the application of the array is that it is deployed in a compact, folded form and put behind the eye, where it then unfolds into its curved, functional form. To be able to manufacture an array with 63 units that all must hinge and fold into the exact correct position would be an incredibly complex task and have many possibilities for error. Thus, it is suggested that the number of units is reduced in the beginning stages of manufacturing.

Collaborators at the Ohio State University plan on using as possibly similar a probe to the transducer design presented in this thesis to begin testing on animal models. This is done by growing ocular melanomas on the eyes of mice and testing the effectiveness and overall safeness of the thermal ablation. It is hoped that if the animal models prove the efficacy of the design, the prototype probe can be used in pre-clinical testing on human patients.

Currently, HIFU technologies are beginning to be more and more widely researched as a method of treating solid tumors. With the results of this project further confirming the ability of HIFU transducers for treating solid tumors, it is hoped that the research being done today is continued and expanded upon. HIFU treatments are considerably safer and pose less risk to the patients than more commonly used cancer treatment methods like radiotherapy, chemotherapy, and invasive surgery. Although this project solely focused on an application of treating ocular melanomas, HIFU technology has the capability of treating a wide array of cancers and is an area that should be continued to be researched.

Chapter 4

CONCLUSION

This thesis focused on the design of a foldable, deployable tessellated Miura-Ori array for the treatment of ocular melanomas. By determining the structural and operating parameters for this array via an analytical model predicting the acoustic pressure field and thermal rises generated, a design was found that could thermally ablate a solid tumor in the eye without harming non-cancerous tissue. Initially, curved rectangular arrays of tessellated Miura-Ori units were tested and it was determined that this structure could not achieve the focusing capabilities for a treatment application. Applying this same analytical framework to an ideal arc transducer, it was found that a transducer arc of ideal focusing met the focusing criteria for ocular melanoma treatment. These results led to the hypothesis that a Miura-Ori array mimicking the hemispherical shape of an ideal arc transducer could be an effective and safe design. After conducting parametric investigations of this array structure, a final design for a hemispherical array was determined with a 15 by 5 unit structure defined by a folding angle of 4˚, edge lengths of 0.175 mm, edge angles of 80˚ and 30˚ respectively, and a driving frequency of 6 MHz. This array structure and operating conditions produced the necessary focusing and temperature rise to safely thermally ablate ocular melanomas.

Further work will focus on the manufacturing of a proof-of-concept probe to be used in pre-clinical testing and animal modeling with collaborators at the Ohio State University. This thesis reaffirms HIFU technology’s treatment capabilities for solid tumors and emphasizes the importance of HIFU research for treating a wide variety of cancers.

REFERENCES

[1] J. E. Kennedy, "High-intensity focused ultrasound in the treatment of solid tumours," *Nat. Rev. Cancer*, vol. 5, pp. 321–327, 2005, doi: 10.1182/blood-2004-10-4135.

[2] G. Malietzis *et al.*, "High-intensity focused ultrasound: Advances in technology and experimental trials support enhanced utility of focused ultrasound surgery in oncology," *Br. J. Radiol.*, vol. 86, no. 1024, pp. 1–12, 2013, doi: 10.1259/bjr.20130044.

[3] D. T. Lynd, C. Zou, J. Crump, and R. L. Harne, "Directive and focused acoustic wave radiation by tessellated transducers with folded curvatures," in *Proceedings of Meetings on Acoustics*, vol. 30, no. 1, Boston, MA, 25-29 June 2017, doi: 10.1121/2.0000667.

[4] R. L. Harne and D. T. Lynd, "Origami acoustics: Using principles of folding structural acoustics for simple and large focusing of sound energy," *Smart Mater. Struct.*, vol. 25, no. 8, pp. 1–11, 2016, doi: 10.1088/0964-1726/25/8/085031.

[5] C. Zou and R. L. Harne, "Tailoring reflected and diffracted wave fields from tessellated acoustic arrays by origami folding," *Wave Motion*, vol. 89, pp. 193–206, Jun. 2019, doi: 10.1016/j.wavemoti.2019.03.001.

[6] C. Zou and R. L. Harne, "Deployable tessellated transducer array for ultrasound focusing and bio-heat generation in a multilayer environment," *Ultrasonics*, vol. 104, May 2020, doi: 10.1016/j.ultras.2020.106108.

[7] K. B. Ocheltree and L. A. Frizzell, "Sound Field Calculation for Rectangular Sources," *IEEE Trans. Ultrason. Ferroelectr. Freq. Control*, vol. 36, no. 2, pp. 242–248, 1989, doi: 10.1109/58.19157.

[8] H. H. Pennes, "Applied Physiology," *J. Appl. Physiol.*, vol. 1, no. 2, pp. 93–1222, 1948, doi: 10.5694/j.1326-5377.1946.tb34690.x.

[9] W. L. Nyborg, "Solutions of the bio-heat transfer equation," *Phys. Med. Biol.*, vol. 33, no. 7, pp. 785–792, 1988, doi: 10.1088/0031-9155/33/7/002.

[10] N. Zhao, “Design and Analysis of Piecewise Assembled , Reconfigurable Acoustic Arrays for Sound Wave Focusing,” MSc Thesis, Dept. of Mech. Eng., The Ohio State Univ., Columbus, OH, 2020.

[11] G. R. Harris, “FDA regulation of clinical high intensity focused ultrasound (HIFU) devices,” in *Proceedings of the 31st Annual International Conference of the IEEE Engineering in Medicine and Biology Society*, Minneapolis, MN, 2-6 Sept. 2009, pp. 145–148, doi: 10.1109/IEMBS.2009.5332444.

[12] C. Zou and R. L. Harne, “Piecewise assembled acoustic arrays based on reconfigurable tessellated structures,” *J. Acoust. Soc. Am.*, vol. 144, no. 4, pp. 2324–2333, 2018, doi: 10.1121/1.5064281.

[13] M. Schenk and S. D. Guest, “Geometry of Miura-folded metamaterials,” *Proc. Natl. Acad. Sci. U. S. A.*, vol. 110, no. 9, pp. 3276–3281, 2013, doi: 10.1073/pnas.1217998110.

[14] R. L. Harne, “Engineering Acoustics : Course Notes.” pp. 1–183, 2021.

[15] C. W. Connor and K. Hynynen, “Bio-acoustic thermal lensing and nonlinear propagation in focused ultrasound surgery using large focal spots: A parametric study,” *Phys. Med. Biol.*, vol. 47, no. 11, pp. 1911–1928, 2002, doi: 10.1088/0031-9155/47/11/306.

[16] D. Rohrbach *et al.*, “Material Properties of Human Ocular Tissue at 7-μm Resolution,” *Ultrason. Imaging*, vol. 39, no. 5, pp. 313–325, 2017, doi: 10.1177/0161734617713498.

[17] H. Tanoue, Y. Hagiwara, K. Kobayashi, and Y. Saijo, “Ultrasonic tissue characterization of prostate biopsy tissues by ultrasound speed microscope,” in *Proc. Annu. Int. Conf. IEEE Eng. Med. Biol. Soc.*, Boston, MA, 30 Aug. - 3 Sept. 2011, pp. 8499–8502, 2011, doi: 10.1109/IEMBS.2011.6092097.

[18] M. Pirtiniçetingl and C. Herman, “Quantification of the thermal signature of a melanoma lesion,” *Int. J. Therm. Sci.*, vol. 50, no. 4, pp. 421–431, 2011, doi: 10.1016/j.ijthermalsci.2010.10.019.

[19] A. S. Song, A. M. Najjar, and K. R. Diller, “Thermally induced apoptosis, necrosis, and heat shock protein expression in 3D culture,” *J. Biomech. Eng.*, vol. 136, no. 7, pp. 1–10, 2014, doi:

10.1115/1.4027272.

[20] W. D. O'Brien *et al.*, "Acoustic output upper limits proposition: Should upper limits be retained?," *J. Ultrasound Med.*, vol. 21, no. 12, pp. 1335–1341, 2002, doi: 10.7863/jum.2002.21.12.1335.

Appendix

Figures A.1a-b: Varying Sphere Angle

Figure A.1a. Sphere angle of 20 degrees

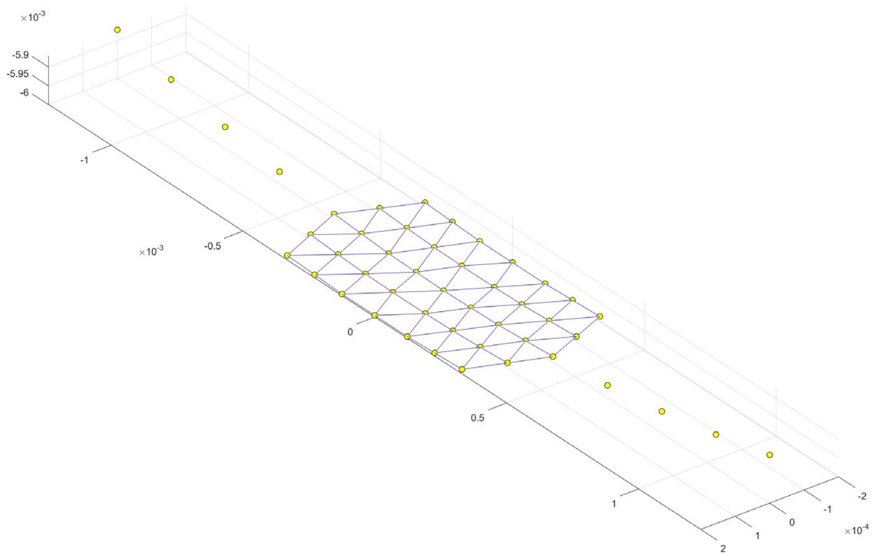

Figure A.1b. Sphere angle of 90 degrees

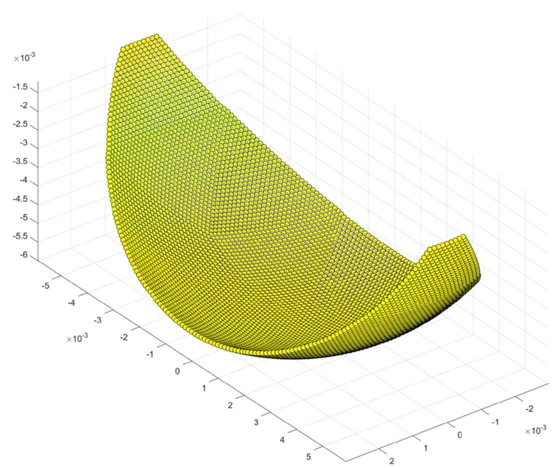

Figures A.2a-b: Varying Scribe Angle 1

Figure A.2a. Scribe Angle 1 of 10 degrees

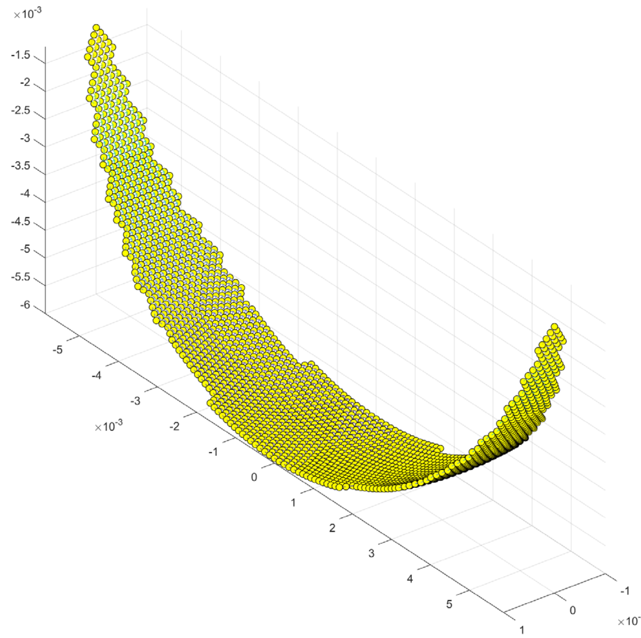

Figure A.2b. Scribe Angle 1 of 90 degrees

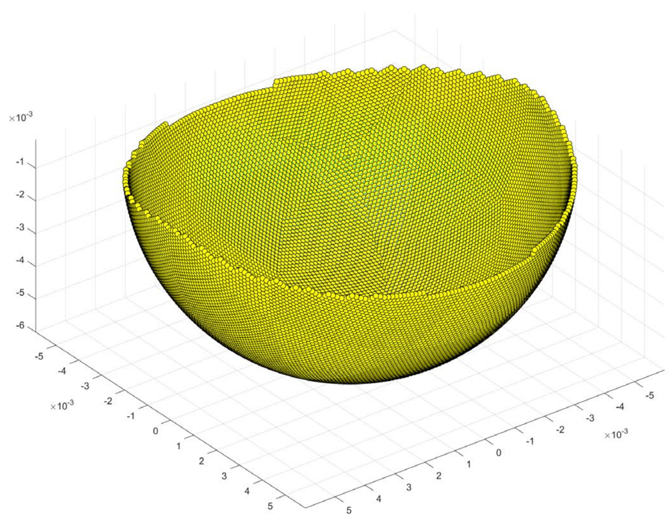

Figures A.3a-b: Varying Scribe Angle 2

Figure A.3a. Scribe Angle 2 of 10 degrees

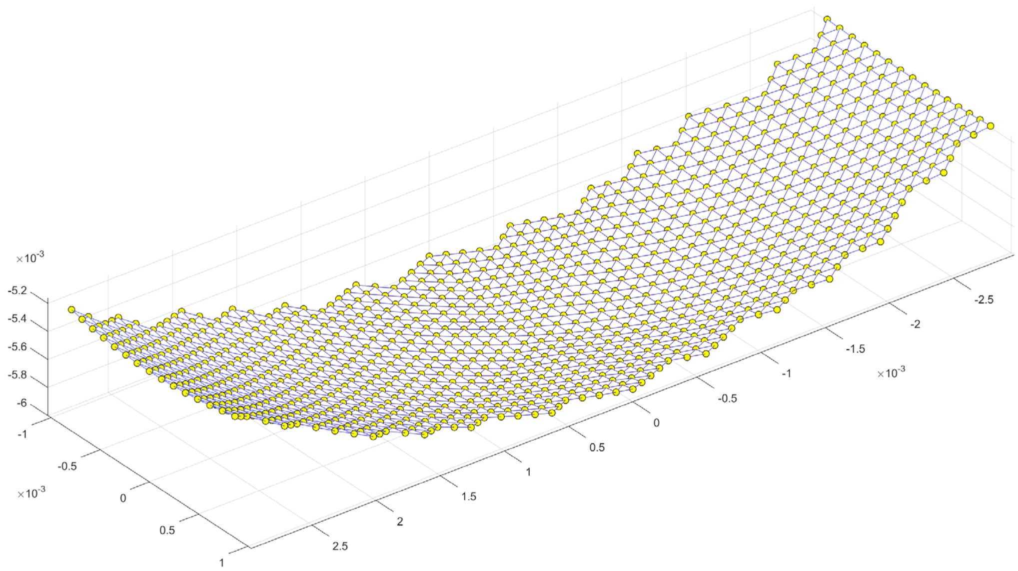

Figure A.3b. Scribe Angle 2 of 90 degrees

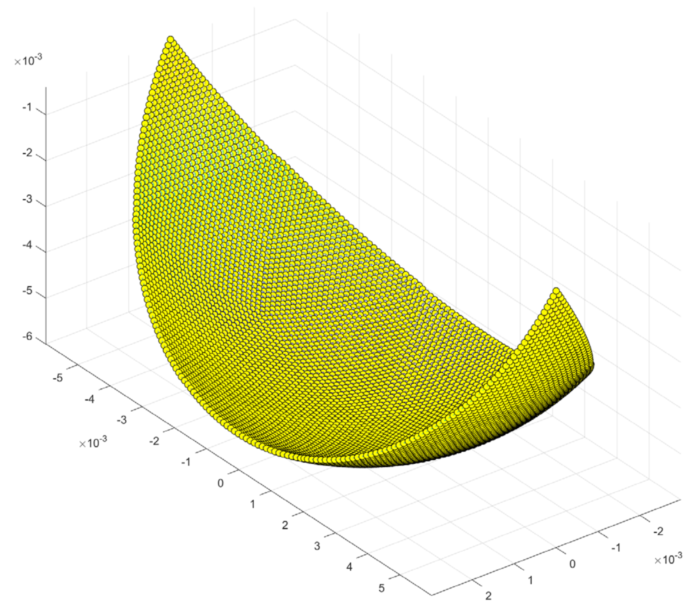

Figures A.4a-b: Varying Radius of Curvature (Variations seen in axis scale rather than shape)

Figure A.4a. Radius of Curvature of 1 mm

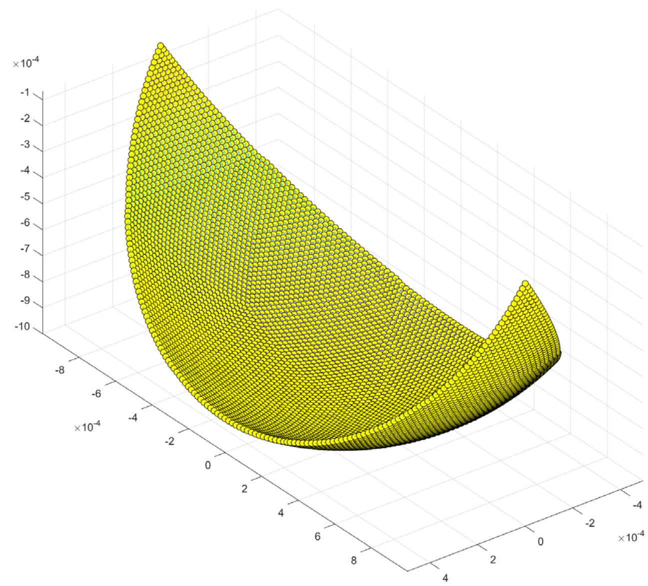

Figure A.4b. Radius of Curvature of 10 mm

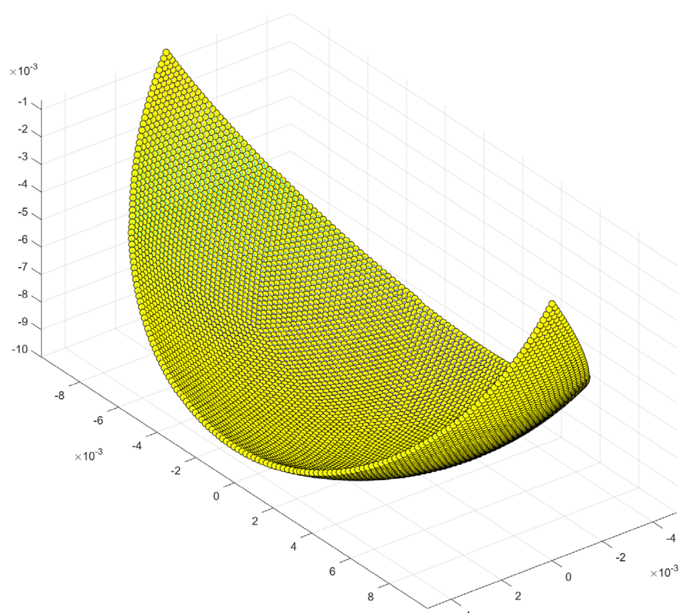

Figure A.5. Acoustic Pressure Plot for Tested Rectangular Miura-Ori Array

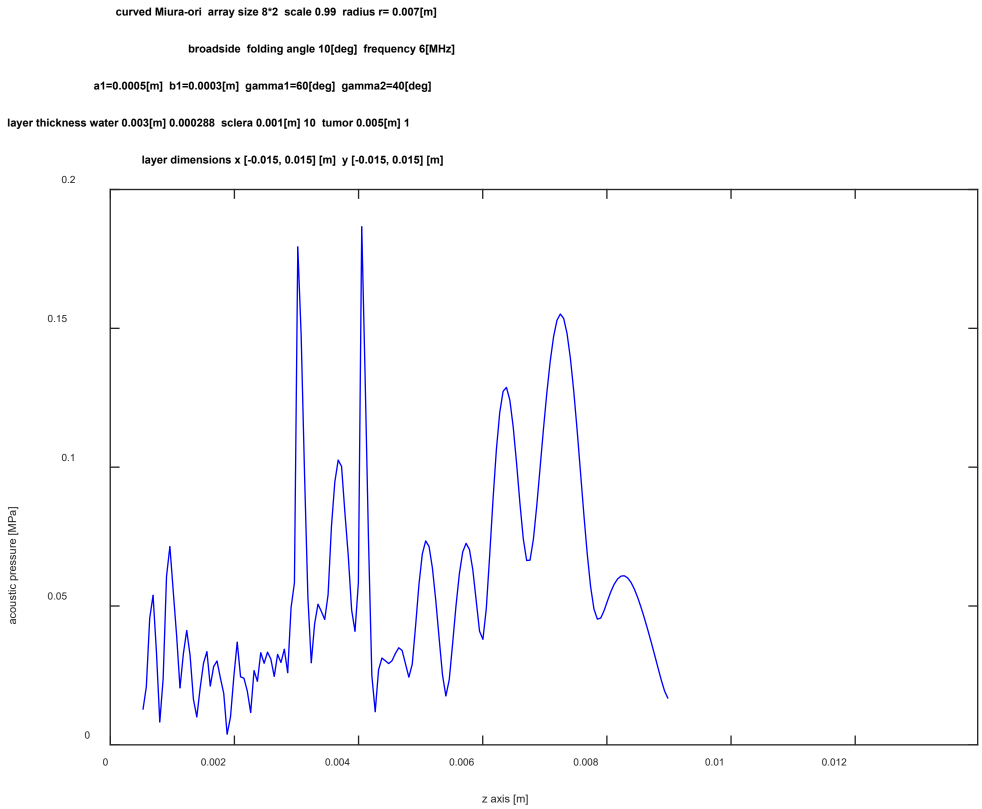

Figure A.6. Acoustic Pressure Plot for Tested Ideal Arc Transducer

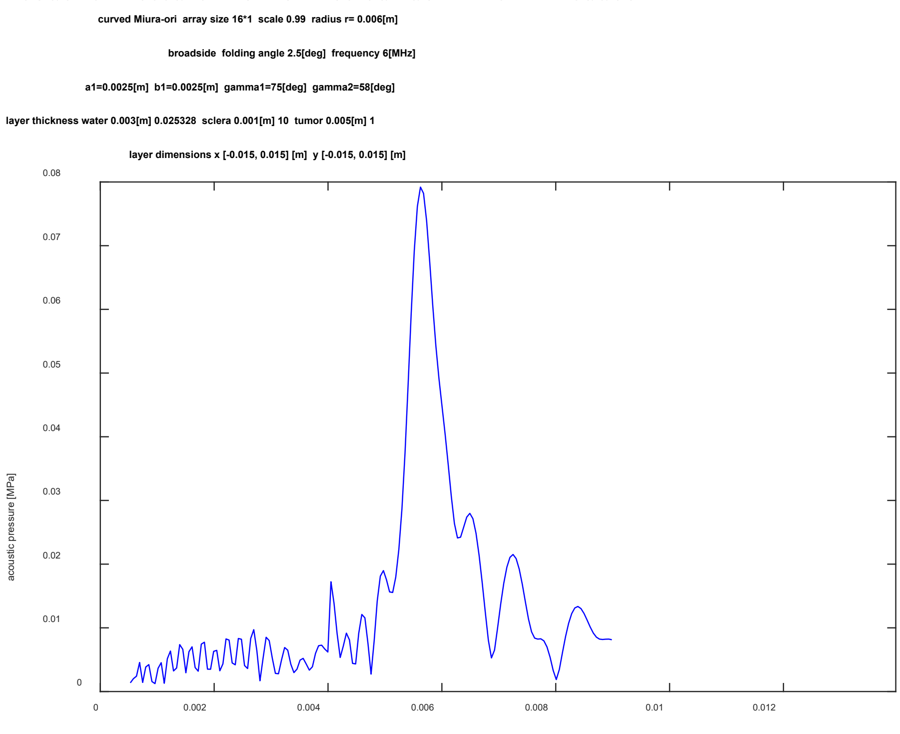

Figure A.7. Acoustic Pressure Plot for Final Design

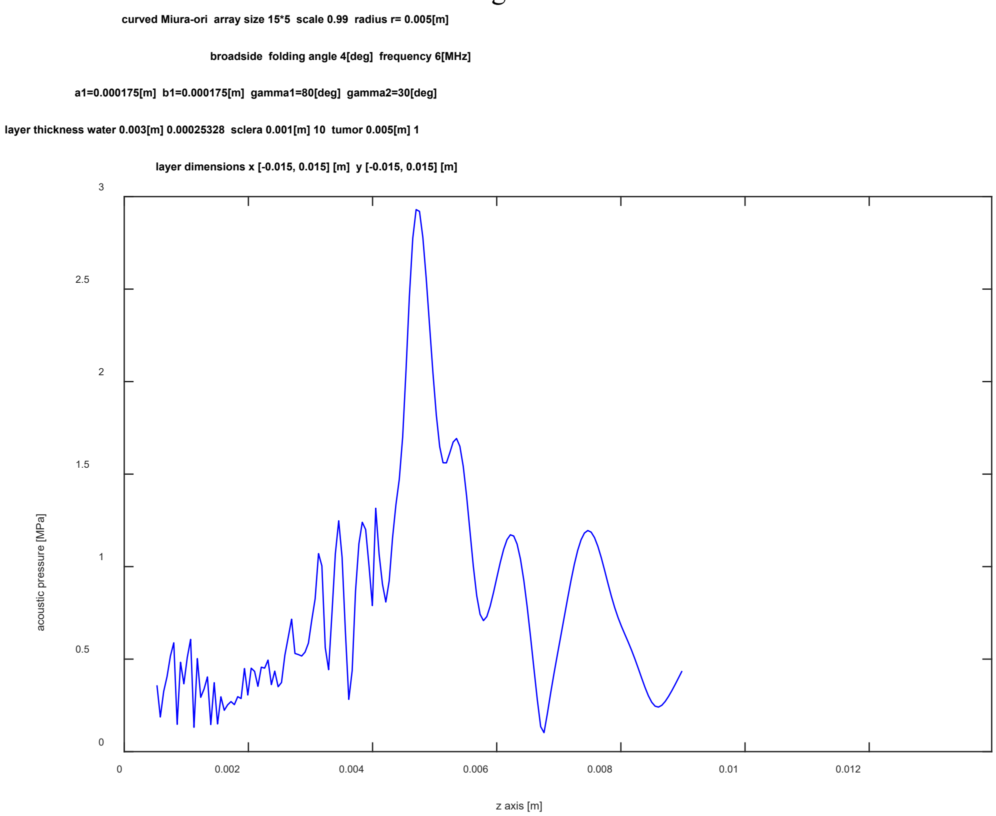

ACADEMIC VITA OF NICHOLAS MOORE

Nicholas Moore | nickmoorenm29@gmail.com | nfm5255@psu.edu

EDUCATION

The Pennsylvania State University Schreyer Honors College — University Park, PA
College of Engineering | Bachelor of Science in Mechanical Engineering — Class of May 2022

PROFESSIONAL EXPERIENCE

Laboratory of Sound and Vibration Research — State College, PA
Undergraduate Researcher — Jan 2020 – present

• Implemented an analytical model in MATLAB to determine the optimal dimensions, driving power, and positioning of a foldable, deployable transducer array to treat ocular melanomas
• Actively determining designs for foldable HIFU transducers for solid tumor treatment by tailoring the dimensions, driving power, and positioning of the transducer via parametric investigations in MATLAB simulations
• Compiled MATLAB results of simulated acoustic and thermal fields generated by HIFU transducer array designs with the goal of completing a thesis in April 2022

LEADERSHIP EXPERIENCE

Alpha Gamma Rho Agricultural Fraternity — University Park, PA
Planning Chair/Junior Planning Chair — Aug 2019 - Present

• Raised over 1000 dollars through managing philanthropic events, risk reduction, and chapter academics to ensure the fraternity's good standing with the university
• Fostered a professional relationship between the university and the fraternity through meetings with Penn State administration to communicate upcoming fraternal events
• Directed the fraternity's 88 members to complete Penn State mandated training programs to educate the organization on risk policies/procedures

Consultant Training Program — University Park, PA
Selected Participant — Sep 2019 – Dec 2019

• Selected from over 100 students to participate in a comprehensive training program that prepares graduates for careers in the consulting industry
• Strengthened core consulting skills through hands-on case study analysis led by Nittany Consulting Group alumni, Penn State faculty, and consulting professionals
• Worked in teams to develop and present solutions to three business cases over the course of the semester testing problem solving in production, marketing, and business structure

SKILLS AND HONORS

Skills: Conversational Spanish, Introductory MATLAB, Proficiency in Microsoft software (Word, PowerPoint), Certified Mental Health First Aider
Honors: Hallowell Engineering Scholarship, Dean's List (5/7), National Merit Finalist, TaeKwon-Do National Silver Medalist